J Mater Sci (2010) 45:552–556
DOI 10.1007/s10853-009-3974-x

Mesolamellar phases containing $[Fe(CN)_6]^{3-}$ anion

Vo Vien · Sung-Jin Kim

Received: 8 July 2009 / Accepted: 10 October 2009 / Published online: 24 October 2009

Abstract The mesostructured lamellar phases with the general formula $[C_nH_{2n+1}N(CH_3)_3]_3[Fe(CN)_6]$ ($n = 14, 16, 18$) were prepared by ion-exchange/precipitation reaction of alkyltrimethylammonium surfactants and $K_3[Fe(CN)_6]$ complex in aqueous medium. The phases were characterized using powder X-ray diffraction, high-resolution transmission electron microscopy, IR spectroscopy, thermogravimetric, and differential scanning calorimetry means. The results obtained all support a proposed model of crystal structure for these materials, in which the layers are constructed by monolayer of the discrete complex molecules, and the surfactants tails of opposite head groups deeply penetrate and arrange with a tilt angle of 63°.

Introduction

The design and synthesis of new solid materials with controlled structures are of great interest in materials science. Since the discovery of a new family of silica mesoporous molecular sieves by scientists at Mobil Oil in 1992 [1], the use of surfactants as structure-directing agents in the synthesis has become a versatile route to various controlled mesoporous materials. It has been well known in ordered silicate mesostructures that lamellar as well as hexagonal and cubic phases could be controlled by using appropriate surfactants and synthesis conditions, and they can be transformed each other [2, 3]. In the case of lamellar phases, increased understanding of supramolecular arrangements in these materials would help us use these surfactant templates more efficiently and design new phases with valuable properties. Therefore, the synthesis of new lamellar phases, structural information on surfactant-based phases, and precise understanding of surfactant–anion interactions in the solid-state have received much attention. Based on the results of the chemistry of mesoporous silicates, recently, the lamellar, hexagonal and cubic phases were also prepared from the molecular clusters [4–9]. However, the chemistry used to construct these frameworks differs from that used in the silicate system. The lamellar phases were obtained predominantly by ion-exchange reaction between the cluster molecules and the surfactants, while the hexagonal and cubic phases were constructed from the cluster building units that are linked together through the metal ions in the template of surfactants. No phase transform between them has been obtained so far [4–9]. These mesostructures based on molecular clusters promise to open new doors to applications in electronic, photonic, and magnetic fields that have been not found in silica framework.

To our knowledge, few works on lamellar phases based on clusters, complexes have been reported. Some of them were characterized by single crystal X-ray diffraction such as $[C_nH_{2n+1}N(CH_3)_3]_4Ge_4Q_{10}$ ($Q = S, Se$; $n = 8–18$) [7, 8], $[C_nH_{2n+1}NH_3]_4Ge_4S_{10}$ ($n = 12–18$) [9], $[C_{12}H_{25}NH_3]_4Sn_2S_6·2H_2O$ [10], $[C_{12}H_{25}N(CH_3)_3]_4H_2V_{10}O_{28}·8H_2O$ [11], $[C_{12}H_{25}N(CH_3)_3]_4V_{12}O_{32}·6H_2O$ [12], $[C_{16}H_{33}N(CH_3)_3]_4SiMo_{12}O_{40}$ [13], $[C_{14}H_{29}N(CH_3)_3]_4[Re_6Te_8(CN)_6]$, $[C_{16}H_{33}N(CH_3)_3]_4[Re_6Se_8(CN)_6]$ [14]. The others that have been described from powder X-ray diffraction and TEM data include $[C_{16}H_{33}N(CH_3)_3]_6(H_2W_{12}O_{40})$, $[C_{16}H_{33}N(CH_3)_3]_{2+x}(Nb_xW_{6-x}O_{19})$ ($x = 2, 3, 4$), [15], $[C_{12}H_{25}N$

V. Vien (✉)
Department of Chemistry, Quy Nhon University, 170 An Duong Vuong street, Quy Nhon City, Vietnam
e-mail: vovien@dng.vnn.vn

S.-J. Kim
Division of Nano Sciences and Department of Chemistry, Ewha Womans University, 120-750 Seoul, Korea

$(CH_3)_3]_6NaPW_{11}O_{39}$ [16], $(NH_4)_x(C_nH_{2n+1}NH_3)_y(NH_4–V_2P_2BO_{12})_6·3H_2O$ ($7 \le n \le 18, x + y = 17$) [17]. However, no works have been reported using $[Fe(CN)_6]^{3-/4-}$ anions in synthesis of ordered mesostructures templated with surfactants. Here, we present the synthesis and properties of a new series of mesostructured materials prepared by an assembly of complex $[Fe(CN)_6]^{3-}$ in the presence of $C_nH_{2n+1}N(CH_3)_3Br$ (n = 14, 16, 18) surfactants.

Experimental

$[C_nH_{2n+1}N(CH_3)_3]_3[Fe(CN)_6]$ (denoted as $C_n–Fe(CN)_6$) phases were prepared by ion-exchange reaction between complex $K_3[Fe(CN)_6]$ and the surfactants in aqueous medium. In a typical synthesis, 0.36 g of the surfactant was dissolved in warm water (5 mL). In a separate flask, 0.1 g of $K_3[Fe(CN)_6]$ were dissolved in 1 mL of H_2O. This solution was added to the surfactant solution. A yellow solid was formed immediately. The mixture was stirred further for 5 h. The solid was isolated by filtration and washed thrice with warm water and dried in air.

Powder X-ray diffraction (PXRD) patterns were obtained with a Rigaku X-ray Diffractometer using Cu–K radiation (λ = 1.5418 Å) at 30 mA and 40 kV. The diffraction data were recorded at scanning rate of 0.12 min^{-1}. Thermogravimetric analysis (TGA) coupled with differential scanning calorimetry (DSC) was carried out on a SETARAM LABSYS TG under nitrogen environment. FT-IR experiments were conducted at room temperature on a ThermoNicolet 6700 spectrometer in the range of wave numbers from 4,000 to 500 cm^{-1} at a resolution of 4 cm^{-1} with 30 scan times. Images of high-resolution transmission electron microscopy (HR-TEM) were achieved with a JEOL JEM-3110.

Results and discussion

The PXRD patterns of the phases reported here are shown in Fig. 1 and clearly reveal their lamellar character. From these diffractions, the interlayer spacing values calculated for $C_{14}–Fe(CN)_6$, $C_{16}–Fe(CN)_6$, and $C_{18}–Fe(CN)_6$ are 23.7, 26.2, and 28.3 Å, respectively. A linear relationship between the interlayer spacing (d) and number of carbon atom (n) of n-alkyl (C_nH_{2n+1} in $C_nH_{2n+1}N(CH_3)_3^+$) has been observed and expressed as $d = 1.15n + 7.67$ (Å) (see Fig. 2). This means that the average increment of the interlayer spacing ($\Delta d/\Delta n$) is 1.15 Å, which is smaller than 1.27 Å for the length increment per carbon atom in a linear all-*trans* chain [18]. Therefore, the alkyl chains of the surfactants in these materials may be arranged as monolayers or deeply penetrate in the interlayer region with a tilt angle of $\sin^{-1}(1.15/1.27) \approx 63°$. Extrapolation of the data to $n = 0$ gives intercept of 7.67 (Å), which is close to the value of diameter of the complex molecule. In fact, this value is smaller than that expected because if $n = 0$, the surfactants become $(CH_3)_3NH^+$. One may be explained by a strong direct anion–cation interaction between the head groups of the surfactant and the complex anions, and that the layers of these phases are constructed from monolayer of the complex anions. The lamellar structures of the materials were confirmed further by high-resolution transmission electron microscopy. Figure 3 shows the TEM image of a representative lamellar phase, $C_{16}–Fe(CN)_6$, with clearly visible layer structures. The interlayer spacing

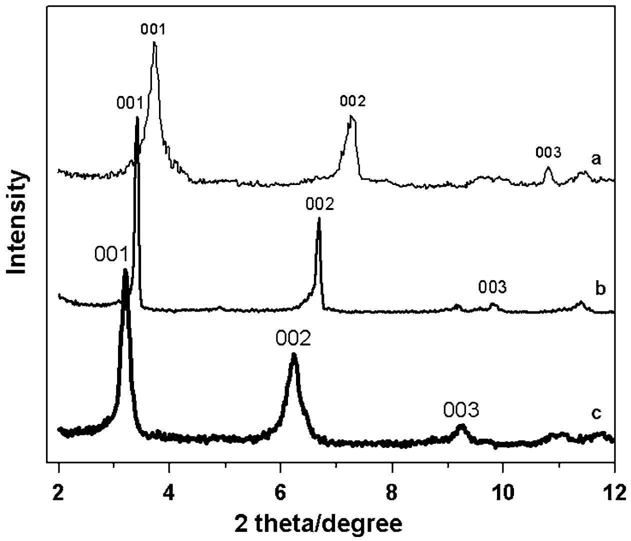

Fig. 1 Powder X-ray diffraction patterns of $C_n–Fe(CN)_6$: n = 14 (*a*), 16 (*b*), 18 (*c*)

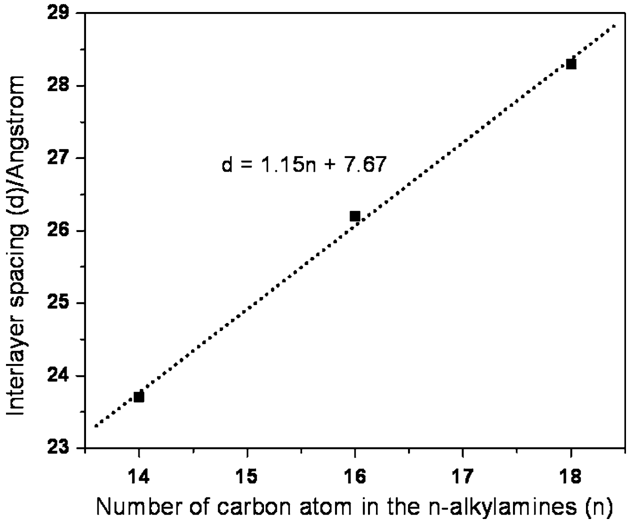

Fig. 2 Plot of inorganic layer-to-layer distance (Å) versus number of carbon atom (n) of n-alkyl (C_n, n = 14, 16, 18) in $C_n–Fe(CN)_6$ phases

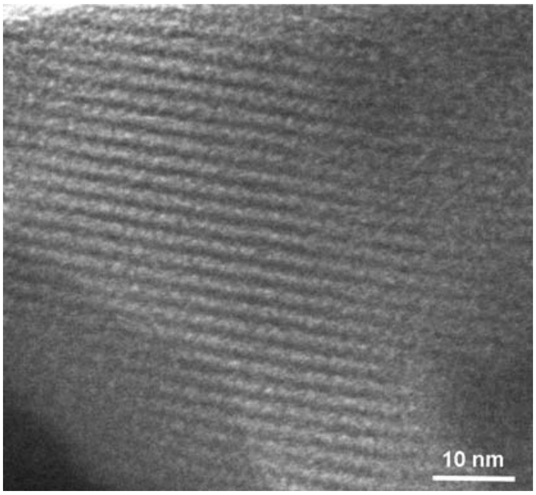

Fig. 3 TEM image of C_{16}–Fe(CN)$_6$

value of the image is about 25.5 Å, which sufficiently matches the *d* value (26.2 Å) obtained from the PXRD data.

To investigate bonding features in the framework of these phases, a representative phase, C_{16}–Fe(CN)$_6$ was characterized by IR and the result was shown in Fig. 4. For comparison, also shown are the IR spectra of complex $K_3[Fe(CN)_6]$ and $C_{16}H_{33}N(CH)_3Br$ (CTABr) surfactant. Figure 4a reveals a characteristic sharp peak at 2,116 cm^{-1} corresponding to the vibration mode of cyanide group of the complex [19]. This peak clearly appears in the spectrum of the material (Fig. 4c). This indicates that cyanide group is intact in C_{16}–Fe(CN)$_6$. It is also shown the presence of CTA in C_{16}–Fe(CN)$_6$ from comparison of the spectrum of CTA (Fig. 4b) and the material (Fig. 4c). In addition, the position of the stretching bands of CH_2 groups is worth to note from the spectra. It is well known that the positions of the antisymmetric stretching band (2,920 cm^{-1}) and the symmetric band (2,850 cm^{-1}) of CH_2 groups in *n*-alkyl chains are sensitive to chain conformation and that these two bands shift to lower wavenumbers if disorder (kink and gauche-blocks) is introduced into the *n*-alkyl chains [20]. In the case of C_{16}–Fe(CN)$_6$, the spectrum exhibits two bands at 2,920 and 2,850 cm^{-1}, which are very close to those of CTA. This means that the *n*-alkyl chains are in ordered conformation in the interlayer space of C_{16}–Fe(CN)$_6$.

The thermochemical properties of C_{16}–Fe(CN)$_6$ were investigated using thermogravimetric analysis coupled with differential scanning calorimetry. Figure 5 indicates that no appreciable weight loss is observed up to 100 °C. The weight loss of the product possesses three steps: the first one around 106 °C (~3%), the second, main step, from 215 to 290 °C (~66%), and the last from 290 to 400 °C (~18%). The first, second, and last may be due to desorption of water, decomposition of the surfactant, and organic residue of the second step, respectively. Total mass loss of the second and last step is about 84%. The DSC curve (Fig. 5) provided an evidence for order and stability of the surfactant tails in the material. Indeed, when heated, the material reveals four endothermal peaks at 70, 106, 268, and 397 °C. As mentioned above, no weight loss happens up to 100 °C; therefore, the first peak can be attributed to a solid phase change. The phase transformation is correlated with increased disorder upon increasing the thermal energy of the surfactant tails in lamellar phases [10, 13, 15]. The second, third, and fourth peak may correspond to desorption of water, decomposition of the

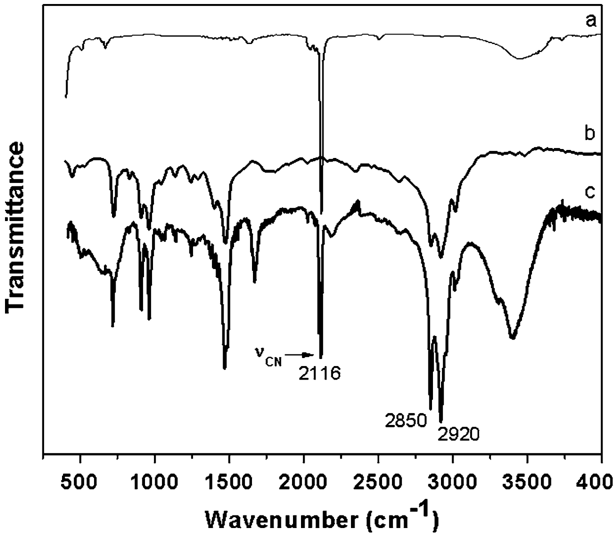

Fig. 4 FTIR spectrum of $K_3[Fe(CN)_6]$ (*a*), CTABr (*b*), and C_{16}–Fe(CN)$_6$ (*c*)

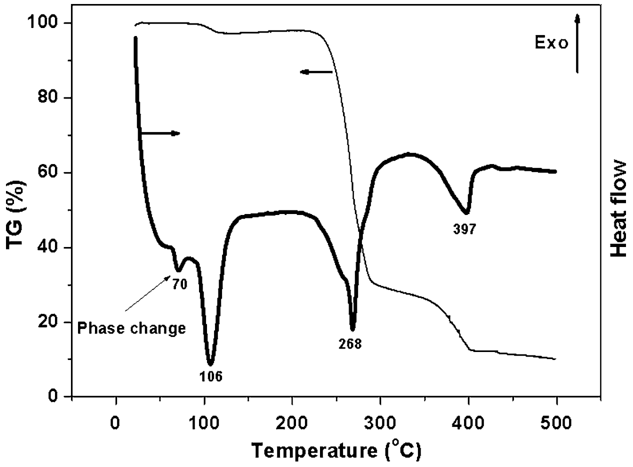

Fig. 5 Thermogravimetric analysis and differential scanning calorimetry of C_{16}–Fe(CN)$_6$

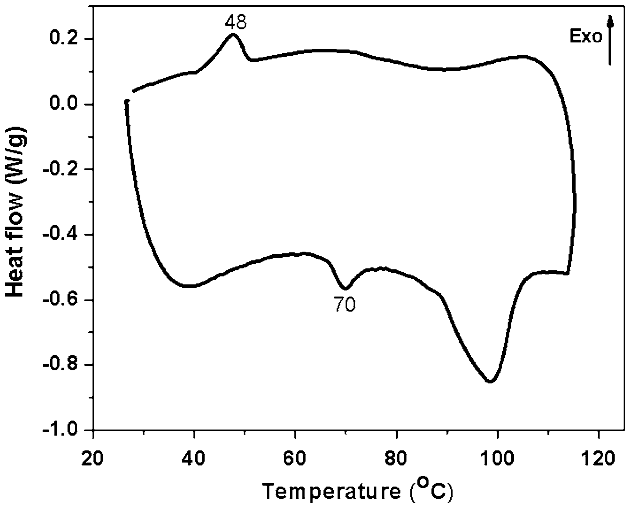

Fig. 6 Differential scanning calorimetry of C_{16}–$Fe(CN)_6$ showing solid-state phase transitions

surfactant, and the organic residue, respectively, as mentioned above. To clarify the phase transformation, C_{16}–$Fe(CN)_6$ was characterized by DSC with heating from room temperature to 115 °C and cooling from 115 °C to room temperature (Fig. 6). When heated, the lamellar phase has an endothermic solid-state phase transition in the region around 70 °C. With cooling, the DSC spectrum of the product shows an exothermic phase change at 48 °C, which likely corresponds with some reordering of the surfactant tails. The sample C_{16}–$Fe(CN)_6$ after the DSC experiment appears unchanged in color and shape. The sample after the DSC experiment was also characterized by PXRD and IR. The results show that the PXRD pattern and IR spectrum are unchanged compared to those of the sample before the DSC experiment. This may indicate that the sample turns to the former phase after the phase change at 48 °C when cooling. The difference between the two phases before and after cooling may be the order of the surfactant tails, and the phase transformations can come from some disordering and reordering of the surfactant tails when changing thermal energy. The phase transformations related to increased disorder upon increasing the thermal energy of the surfactant tails in lamellar phases were reported in the previous articles [10, 13, 15].

A combination of the IR, EDX, elemental C, H, N, and TGA analysis supports a chemical formula of C_n–$Fe(CN)_6$ to be $[C_nH_{2n+1}N(CH_3)_3]_3[Fe(CN)_6]$. The type of this formula was also observed in most of the lamellar phases prepared from the cluster and the surfactants, and it as a result comes from cationic exchange reaction [7–17]. The structure of these lamellar phases is suggested by a model shown in Fig. 7.

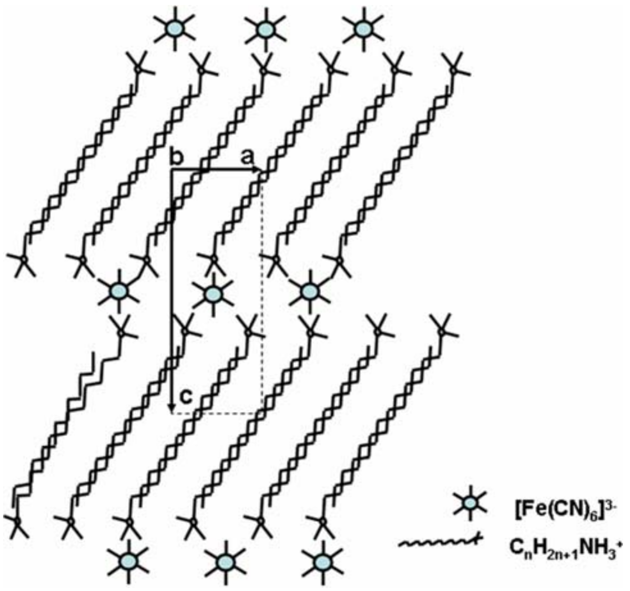

Fig. 7 A model illustrates the structure of C_n–$Fe(CN)_6$

Conclusion

In summary, the results obtained here show that the assembly of complex $K_3[Fe(CN)_6]$ in the presence of $C_nH_{2n+1}N(CH_3)_3Br$ ($n = 14, 16, 18$) surfactants yields a series of new, highly ordered lamellar phases. These phases possess the layers that are constructed by monolayer of the discrete complex molecules, and in their interlayer region, the surfactant tails of opposite heads deeply penetrate and arrange with a tilt angle of 63°.

Acknowledgements This work was supported by National Foundation for Science and Technology Development (NAFOSTED, 104.03.06.09), and by National Research Foundation of Korea Grant funded by the Korean Government (20090063004) and Seoul R&BD Program (10816).

References

1. Kresge CT, Leonowicz M, Roth WJ, Vartuli JC, Beck JC (1992) Nature 359:710
2. Huo Q, Margolese DI, Stucky GD (1996) Chem Mater 8:1147
3. Lee HI, Pak C, Yi SH, Shon JK, Kim SS, So BG, Chang H, Yie JE, Kwon YU, Kim JM (2005) J Mater Chem 15:4711
4. MacLachlan MJ, Coombs N, Ozin GA (1999) Nature 397:681
5. Trikalitis PN, Rangan KK, Bakas T, Kanatzidis MG (2001) Nature 410:671
6. Korlann SD, Riley AE, Kirsch BL, Mun BS, Tolbert SH (2005) J Am Chem Soc 127:12516
7. Bonhomme F, Kanatzidis MG (1998) Chem Mater 10:1153
8. Wachhold M, Kanatzidis MG (2000) Chem Mater 12:2914
9. Rangan KK, Kanatzidis MG (2004) Inorg Chim Acta 357:4036
10. Li J, Marler B, Kessler H, Soulard M, Kallus S (1997) Inorg Chem 36:4697

11. Janauer GG, Dobley AD, Zavalij PY, Whittingham MS (1997) Chem Mater 9:647
12. Janauer GG, Dobley A, Guo J, Zavalij P, Whittingham MS (1996) Chem Mater 8:2096
13. Nyman M, Ingersoll D, Singh S, Bonhomme F, Alam TM, Brinker CJ, Rodriguez MA (2005) Chem Mater 17:2885
14. Suh MJ, Vien V, Huh S, Kim YM, Kim SJ (2008) Eur J Inorg Chem 686
15. Stein A, Fendorf M, Jarvie TP, Mueller KT, Benesi AJ, Mallouk TE (1995) Chem Mater 7:304
16. Taguchi A, Abe T, Iwamoto M (1998) Micropor Mesopor Mater 21:387
17. Do J, Jacobson AJ (2001) Chem Mater 13:2436
18. Kitaigorodskii AI (1973) Molecular crystals and molecules. Academic Press, New York
19. Bennett MV, Beauvais LG, Shores MP, Long JR (2001) J Am Chem Soc 123:8022
20. Vaia RA, Teukolsky RK, Giannelis EP (1994) Chem Mater 6:1017